Electronic Supplementary Information (ESI) for Chem.Commun.

This journal is © The Royal Society of Chemistry 2021

Electronic Supplementary Information for

Direct visualization of photo-induced disulfide through oxidative coupling of *para*-aminothiophenol

Wei He, [a, b] Chang Xia, [c] Peng Fei Gao, [a] Jun Zhou, [a] Yuan Fang Li, *[c] and Cheng Zhi Huang*[a]

a. Key Laboratory of Luminescence Analysis and Molecular Sensing (Southwest University), Ministry of Education College of Pharmaceutical Sciences, Southwest University, Chongqing 400715 (P. R. China). E-mail: chengzhi@swu.edu.cn

b. Chongqing Key Laboratory of Inorganic Special Functional Materials, College of Chemistry and Chemical Engineering, Yangtze Normal University, Chongqing 408100, (P. R. China)

c. Key Laboratory of Luminescent and Real-Time Analytical System (Southwest University), Chongqing Science and Technology Bureau, College of Chemistry and Chemical Engineering, Southwest University, Chongqing 400715, P. R. China. liyf@swu.edu.cn

Experimental section

Materials and Reagents.

para-aminothiophenol (*p*-ATP, >98%) and *para*-nitrothiophenol (*p*-NTP, >95%) were purchased from TCI (Shanghai) Development Co., Ltd. (Shanghai, China). 4-amino phenyldisulfide (APDS, >98%) was obtained from Aladdin (Shanghai, China). 5,5′-dimethyl-1-pyrroline-N-oxide (DMPO) was purchased from Sigma-Aldrich (Shanghai, China). Hydrochloric acid, sodium hydroxide used to adjust the pH of the solution were obtained from Chuandong Reagent Co., Ltd. (Chongqing, China). All reagents were used as received. Ultrapure water (18.2 MΩ) was utilized from a Milli-Q system (Millipore, Bedford, MA, USA). Glass slides were commercially purchased from Ted Pella, Inc. (California, USA).

Apparatus.

Ultraviolet-visible absorption spectra were measured by a U-3010 spectrometer (Hitachi, Japan). The morphology of the organic nanoparticles was imaged by S-4800 field-emission scanning electron microscope (Hitachi, Japan). Light scattering DFM images were captured by dark-field imaging system, which was equipped with optical microscope (BX53, Olympus, Japan), a DP72 single chip true-color charge coupled device (CCD) camera (Olympus, Japan) and halogen light source (100 W, U-LH100-3). High numerical aperture dark-field condenser (U-DCW, NA=1.2−1.4) and 100 magnification oil immersion objective lens were used in the imaging. Image-Pro Plus (IPP) 6.0 software (Media Cybernetics, USA) was utilized to analyze the intensity of scattering spots in dark-field images. Raman spectra were conducted on a LabRAM HR800 spectrometer with a laser of 532 nm (Horiba Jobin-Yvon, France). High-resolution mass spectra (HRMS, ESI-Q-TOF) were recorded on Bruker impact-II (Bruker, Germany). EPR spectra were recorded at room temperature using Bruker A300-10/12 EPR spectrometer (Bruker, Germany). The transient absorption spectra were conducted with home-built pump-probe setup[1], the excitation laser pulses comes from an optical parametric amplifier (TOPAS Prime, Spectra Physics) pumped by a Ti:Sapphire femtosecond laser (35fs, 800 nm, 1 kHz, Spectra Physics) and spectra were collected by a fiber optical spectrometer (AvaSpec-ULS2048CL-EVO, Avantes).

Real time monitoring the photooxidative coupling reaction by DFM

The nanoparticle-forming photooxidative coupling reaction was monitored by light scattering dark-field microscopy (DFM). Firstly, the flow reaction cell was made by using pre-cleaned glass microscope slide labeled with light cross scratches and glass coverslip[2]. After washed by ultrapure water and dried by N_2, the reaction cell was placed on the dark-field microscope and representative black area near the cross was selected for imaging. After taking the original background DFM image in the pure solvent (water or ethanol), 200 μL *p*-ATP or *p*-NTP solution was added to the flow cell to initiate the photooxidative coupling reaction under the irradiation of the light source of the microscope, and the reaction was monitored *in situ* and in real time through a series of DFM images in the same area with a certain time interval.

Characterization the morphology of organic nanoparticles

The co-localization technique of DFM image and SEM image was employed to track the morphological of organic nanoparticles by observing the same nanoparticles in the area near the cross. When the photooxidative reaction was stopped, the glass slide was washed with ultrapure water to remove the unreacted *p*-ATP solution and dried by N_2 by gentle operation. Then the glass slide was vacuum sputtered 15 seconds for SEM characterization.

Monitoring the photooxidative coupling reaction with various light sources

The whole sandwich reaction cell with 200 μL *p*-ATP aqueous solution was irradiated by various light sources such as halogen lamp of dark-field microscope (100 W) without passing through the condenser, which is named as unfocused irradiation condition, ultraviolet light of 365 nm (12 W), Xenon lamp (300 W, with a 400 nm cutoff filter) and sunlight for 1 hour, then free *p*-ATP molecules were washed away by the ultrapure water and the remained organic nanoparticles on the substrate were observed by DFM images in water medium, finally the morphology of organic nanoparticles were characterized by SEM.

Preparation solid product of the photooxidative coupling reaction

4 mL 10 mM *p*-ATP ethanol/water solution in quartz cuvette (10 mm × 10 mm) was irradiated with the Xenon lamp (300 W, with a 400 nm cutoff filter) for 4 hours, the solution became turbid and finally the photoproducts were flocculated and precipitated as solids at the bottom of the cuvette because of their poor solubility in water. After taking out the

supernatant carefully, the precipitation was dried by lyophilization for further characterization by HRMS and Raman spectra.

Normal Raman spectra measurement of the photoproduct and *p*-ATP solution

The obtained photoproduct was placed on the silicon wafer for normal Raman spectra measurement through a Raman microscope system. The *p*-ATP aqueous solution or *p*-ATP ethanol solution was placed in the glass capillary tube for in situ normal Raman measurements for monitoring the photooxidative coupling reaction with 532 nm laser irradiation.

Supporting Results and Discussion

Effect of exposure time on light scattering intensity of nanoparticle on the DFM images

The light scattering intensity of nanoparticle in DFM image was mainly dependent on the diameter of nanoparticle itself in the same imaging experimental condition such as exposure time, so in the process of monitoring the photooxidative coupling reaction of *p*-ATP, the light scattering intensity of nanoparticle increased accompanying with the increasing diameter (Fig. S2, ESI†).

The light scattering intensity of nanoparticle in DFM image was also dependent on the exposure time when images were captured. Generally speaking, the scattering intensity of the same nanoparticles increased when the imaging exposure time was prolonged (Fig. S2, ESI†). However, too long exposure time may produce background scattering intensity and interference between nanoparticles, as Fig. S1 shows, so exposure time should be adapted to make compromise between the scattering intensity of nanoparticles and signal-to-noise ratio. That is to say, short exposure time is more suitable for large nanoparticle with strong scattering light, vice versa, long exposure time is more suitable for small nanoparticle with weak scattering light. However, when contrast experiments of various influencing factors were made, the exposure time should be kept consistent for comparison.

Difference of reaction mechanism between disulfide-coupling and azo-coupling

When *p*-ATP and *p*-NTP are converted to DMAB as model reaction on the surface of metal nanoparticles such as gold and silver nanoparticles, both *p*-ATP and *p*-NTP are chemically combined to the surface of metal nanoparticles through gold-sulfur bond or silver-

sulfur bond to form self-assembled monolayer, wherein the reactive site of the sulfhydryl function group is blocked, meanwhile the plasmon-assisted photocatalytic coupling reaction take place on the retained amino groups (oxidative coupling) and nitro groups (reductive coupling) to form azo-dimerization DMAB through photo-induced hot-carriers.[3-5] Under our experimental conditions, however, both the amino, nitro and sulfhydryl function group are active sites, the sulfhydryl group takes precedence over the amino and nitro groups to undergo photo-oxidative coupling reaction to form disulfides (APDS or NPDS) rather than DMAB. In such case, the selective oxidative-coupling of p-ATP in aqueous medium has the following mechanism to produce disulfide APDS through photochemical reaction.

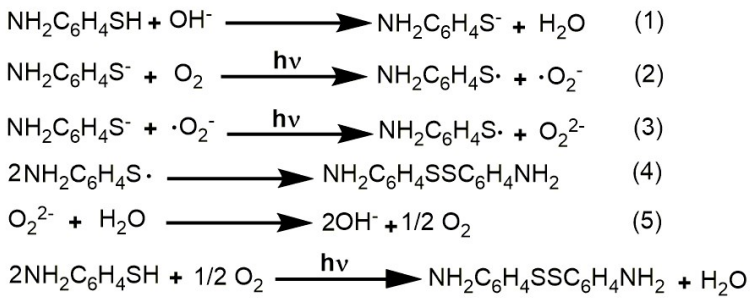

Normal Raman spectra of the *p*-ATP solution

The normal Raman scattering signal of *p*-ATP solution is too weak to be detected even if the concentration of the solution was increased to 1 mM, which is easily interfered by the Raman scattering signal of solvent such as ethanol, and there is no obvious change in normal Raman spectra when *p*-ATP solution was irradiated by 532 nm laser in Raman spectrometer continuously (Fig. S18, ESI†). Therefore, the normal Raman spectroscopy failed to monitor the photochemical reaction of *p*-ATP solution alone in the absence of surface-enhanced Raman scattering (SERS) substrate such as gold or silver nanoparticles, that is why we used DFM instead of normal Raman spectroscopy for monitoring the photochemical reaction of *p*-ATP solution in real time.

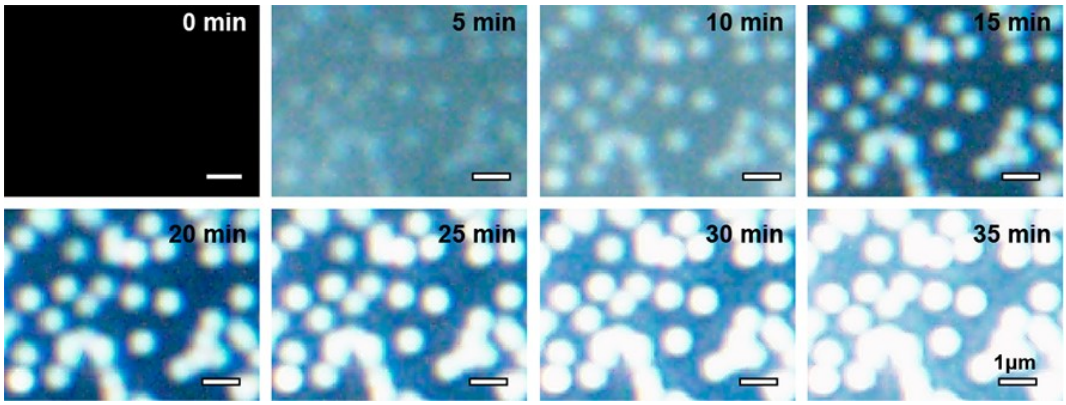

Figure S1 Monitoring photooxidative coupling reaction of *p*-ATP with increased exposure time, exposure time, 3.5 s, $c_{p\text{-ATP}}$, 1×10^{-4} mol·L^{-1}.

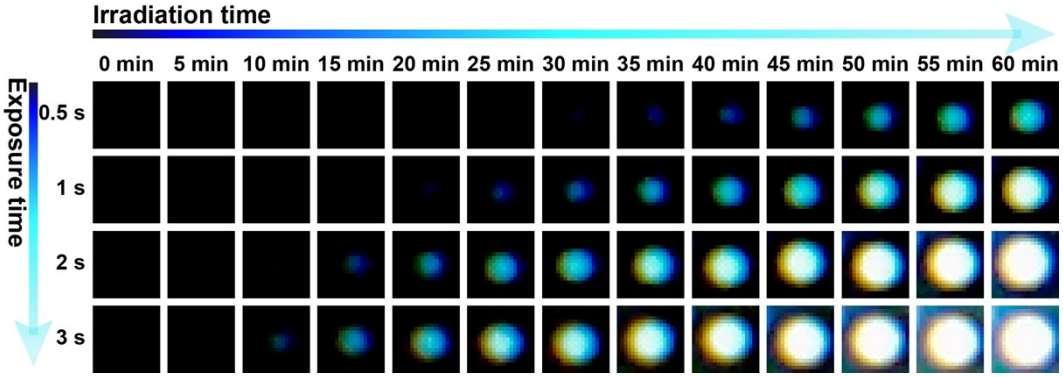

Figure S2 The effect of exposure time on DFM images of single organic nanoparticle in the process of photooxidative coupling reaction. All images are captured from the same organic nanoparticle at different exposure time (0.5–3 s) and irradiation time (0–60 min). $c_{p\text{-ATP}}$, 5×10^{-5} mol·L^{-1}.

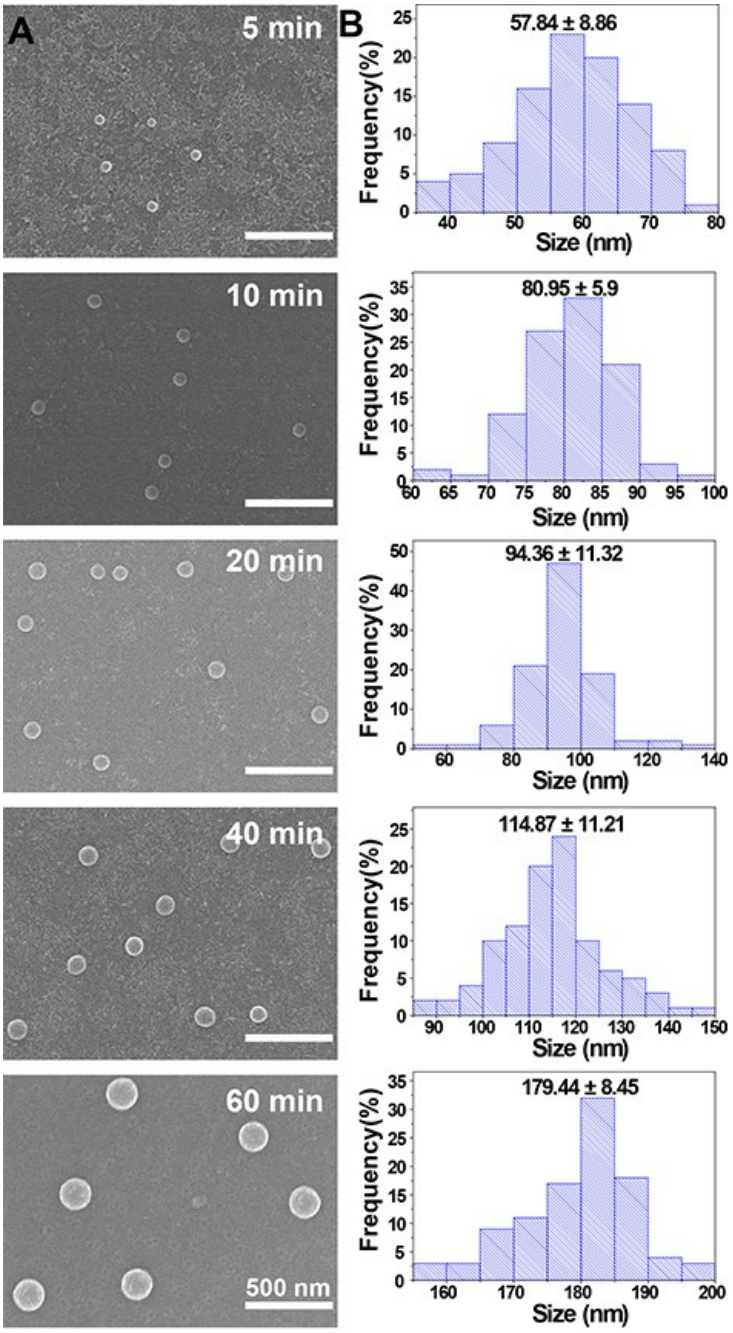

Figure S3 SEM images (A) and size distribution histograms (B) of organic nanoparticles obtained by different irradiation times. (n = 100)

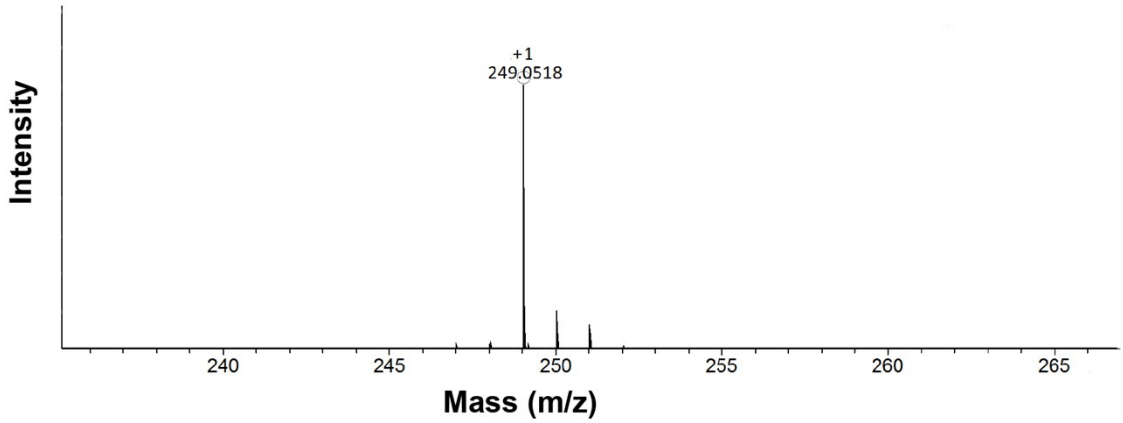

Figure S4 High-resolution mass spectra of the solid photoproduct produced by irradiation of *p*-ATP aqueous solution.

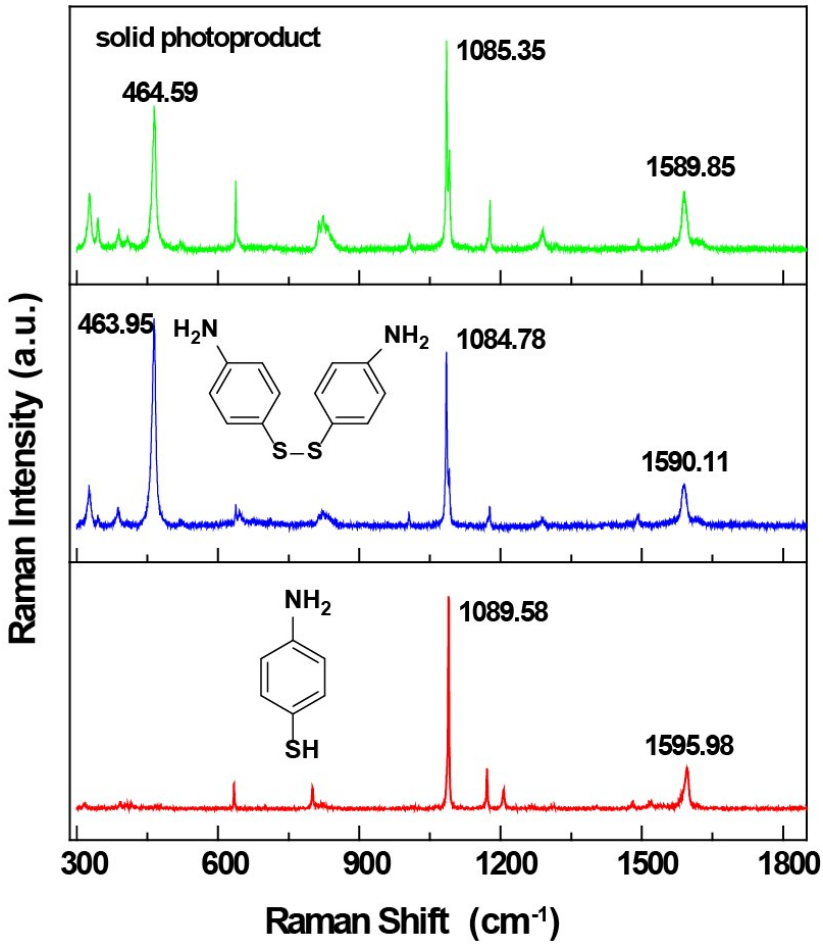

Figure S5 Normal Raman spectra of the solid photoproduct produced by irradiation of *p*-ATP aqueous solution and solid power of APDS and *p*-ATP.

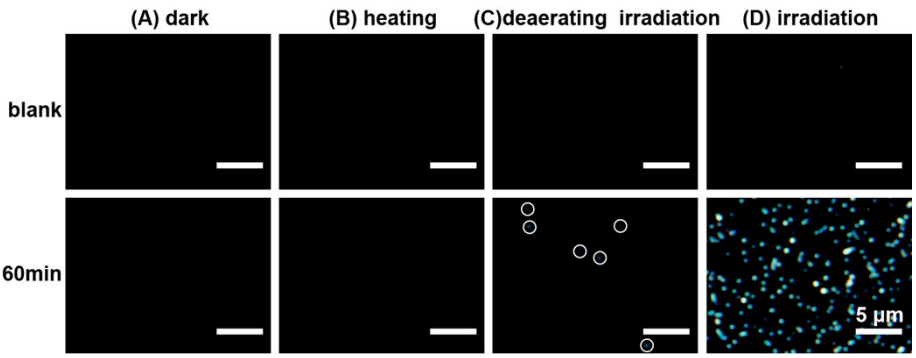

Figure S6 Control experiments confirmed the critical role of irradiation and dissolved oxygen. DFM images of the *p*-ATP aqueous solution placed in the dark (A), heated in 60 ℃ water bath (B), deaerating with N_2 for 15min then irradiation (C) and irradiation (D) for the same time of 60min. The white circle in figure (C) indicated the nanoparticles formed. The blank images were captured in the same area in water medium before adding the *p*-ATP solution to reduce the interference of impurities on the slide. $c_{p\text{-ATP}}$, 2×10^{-5} mol·L^{-1}, exposure time, 3 s.

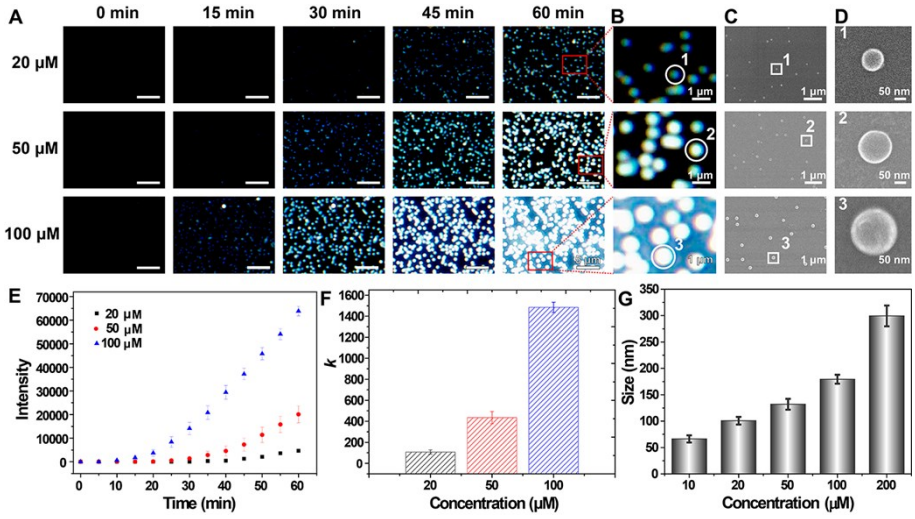

Figure S7 The effect of concentration of *p*-ATP aqueous solution on photooxidative coupling reaction. (A) The dynamic DFM images with different concentrations captured at different time, scale bar, 5 μm. (B) Enlarged DFM images labeled with red frame in Fig. A. (C) SEM images of the co-localization region in Fig. B. (D) Magnified SEM image of single nanoparticle labeled with 1-3 in Fig. C. (E) Concentration dependent scattering intensity evolution. Error bars are calculated from 5 particles in Figure A. (F) Concentration dependent photocoupling reaction rate constants of *p*-ATP solution. (G) The effect of concentration on the diameter of organic nanoparticles obtained by irradiation for 60 min.

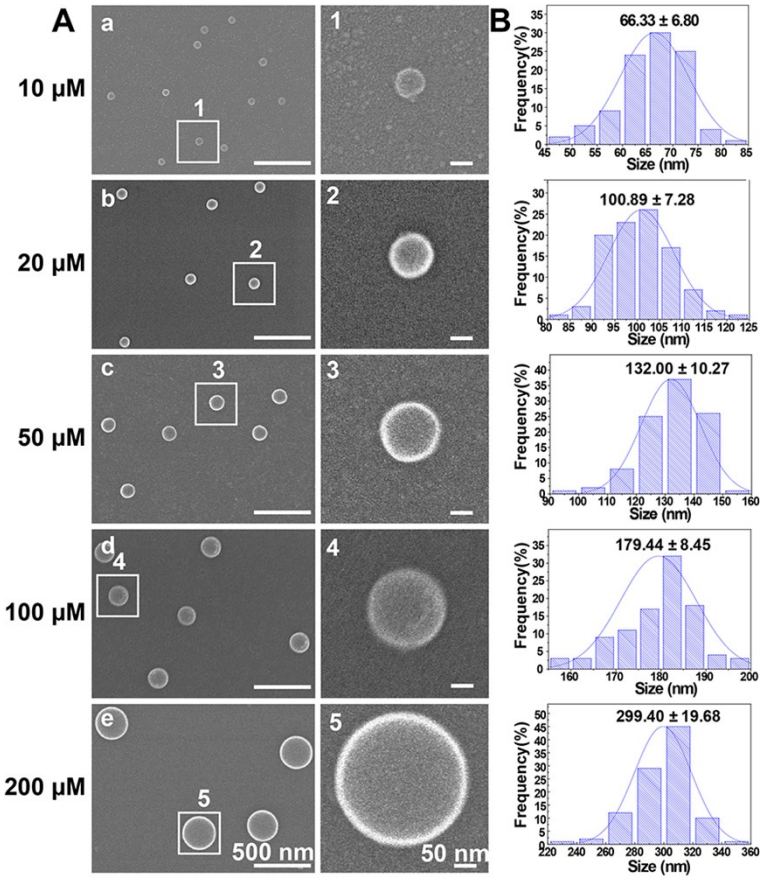

Figure S8 SEM images (A) and size statistics (B) of organic nanoparticles formed by irradiation of different concentration of *p*-ATP aqueous solution for 60 min (n = 100).

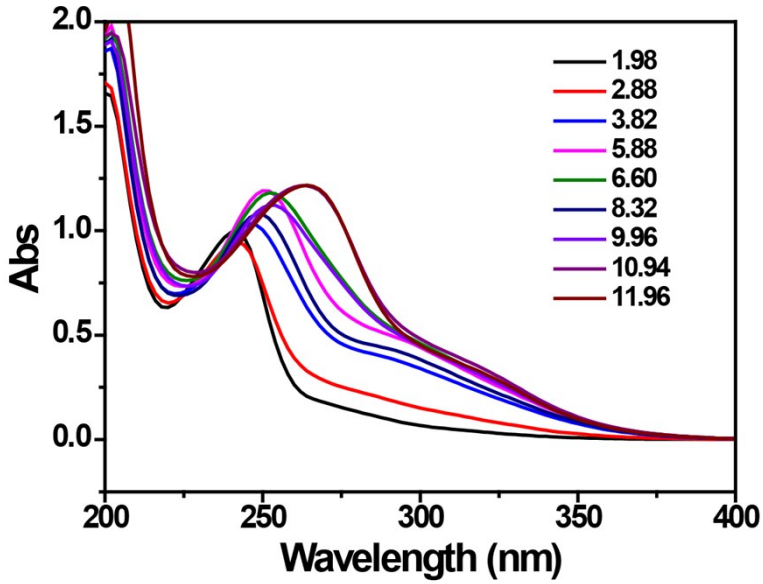

Figure S9 Ultraviolet-visible absorption spectra of *p*-ATP aqueous solution with different pH, $c_{p\text{-ATP}}$, 2.5 × 10^{-4} mol·L^{-1}.

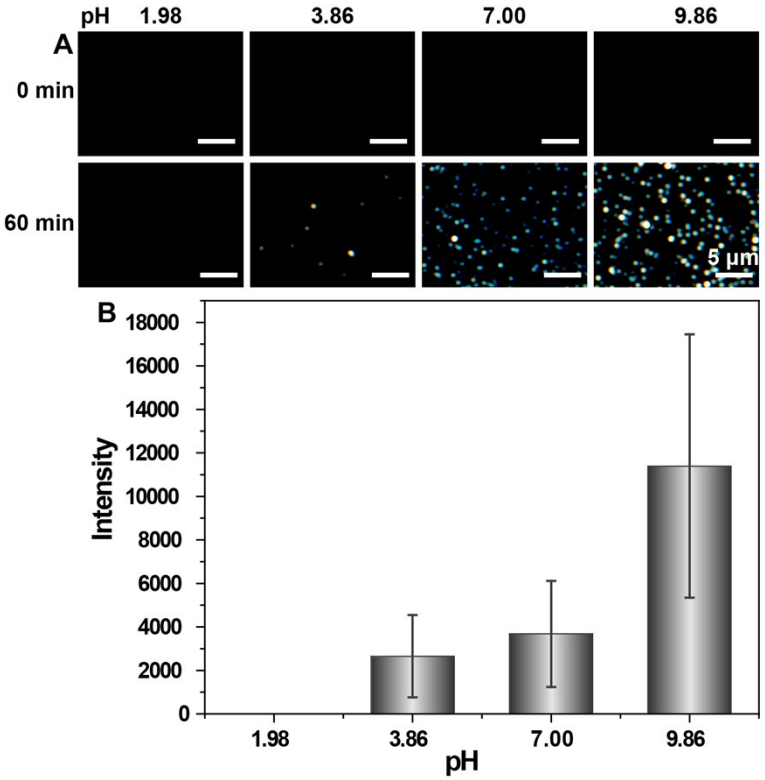

Figure S10 The effect of pH on photooxidative coupling reaction of *p*-ATP aqueous solution. (A) DFM images of *p*-ATP solution with different pH values before and after irradiation for 60min. (B) Scattering intensity analysis of 50 organic nanoparticles shown in figure A at different pH value. $c_{p\text{-ATP}}$, 2×10^{-5} mol·L^{-1}, exposure time, 3 s.

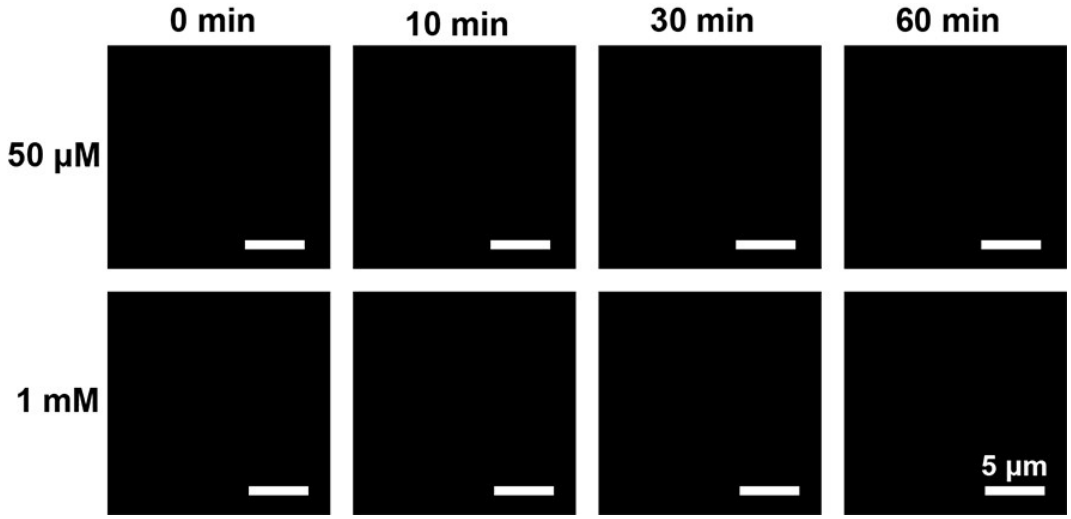

Figure S11 DFM images of *p*-ATP ethanol solution at different irradiation time, exposure time, 3 s.

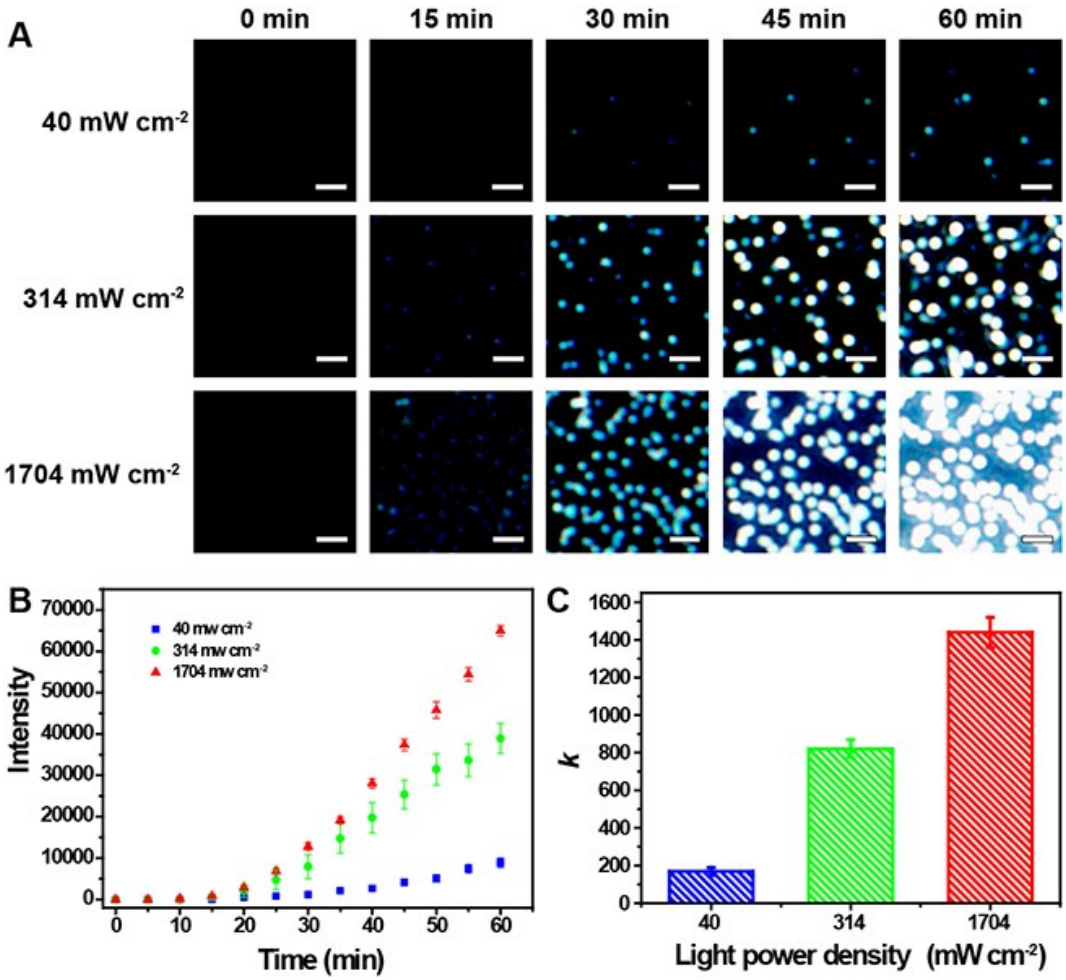

Figure S12 Light power density dependence of photooxidative coupling reaction. (A) The dynamic DFM images of *p*-ATP aqueous solution irradiated with different light powers density at different time, scale bar, 2 μm. (B) Scattering intensity evolution of organic nanoparticles with different light powers density. (C) Dependence of photocoupling reaction rate constants on light power density. $c_{p\text{-ATP}}$, 1×10^{-4} mol·L^{-1}, exposure time, 1s.

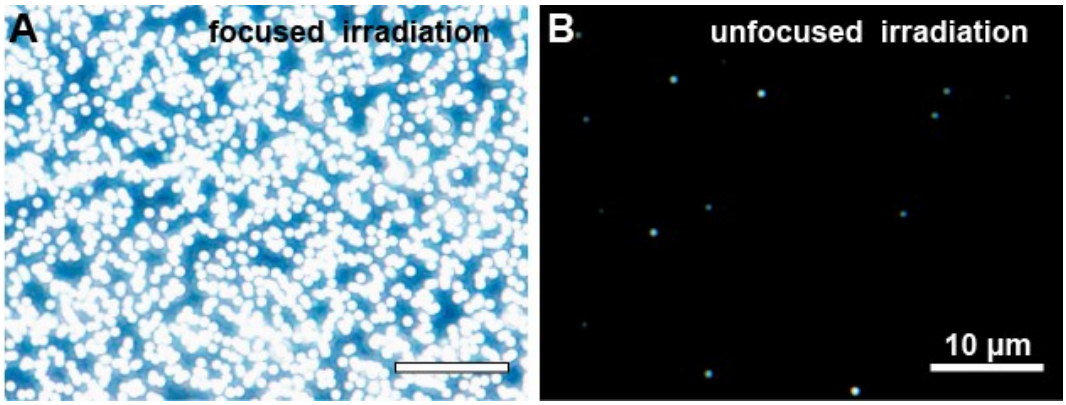

Figure S13 The effect of focused and unfocused conditions on photooxidative coupling reaction. DFM images of *p*-ATP aqueous solution by focused irradiation (A) and unfocused irradiation (B) from 100 W halogen lamp of dark-field microscope for 60 min, $c_{p\text{-ATP}}$, 1×10^{-4} mol·L^{-1}.

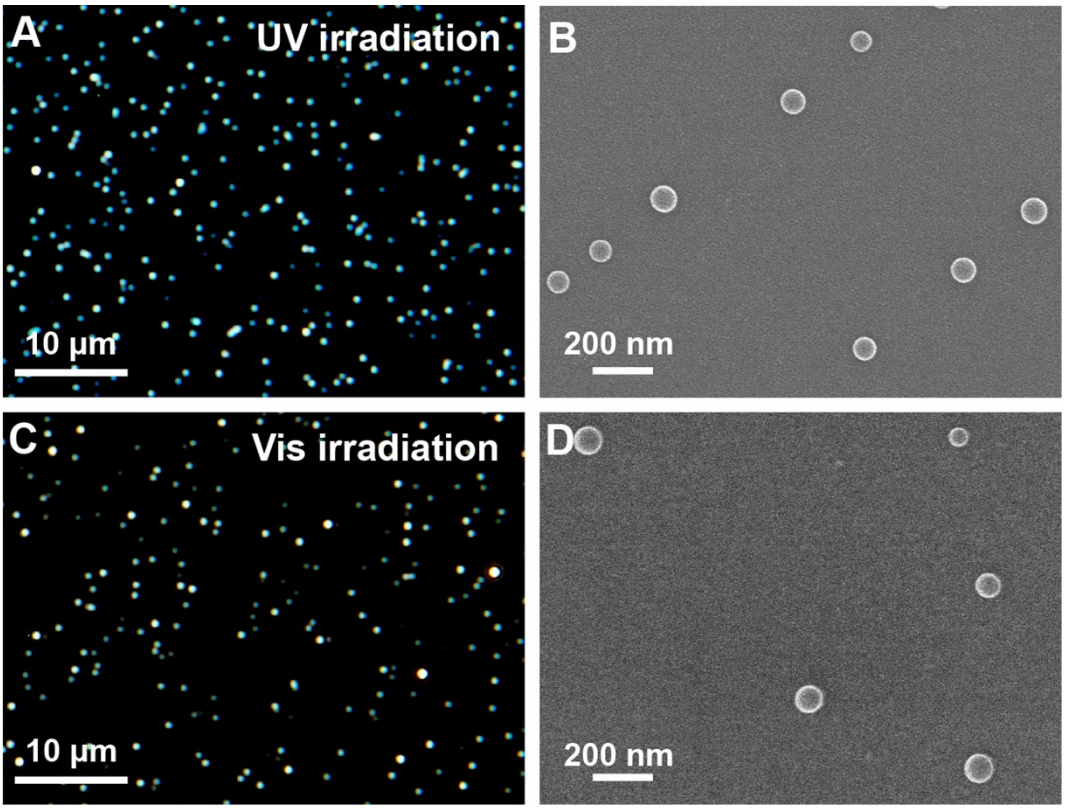

Figure S14 The universality of light sources with different wavelength on the photooxidative coupling reaction. DFM images and SEM images of disulfide organic nanoparticles formed by irradiation *p*-ATP aqueous solution with 365 nm UV lamp (A, B) and Xenon lamp (300 W, with a 400 nm cutoff filter, C, D) for 60 min. $c_{p\text{-ATP}}$, 1×10^{-4} mol·L^{-1}. exposure time, 3 s.

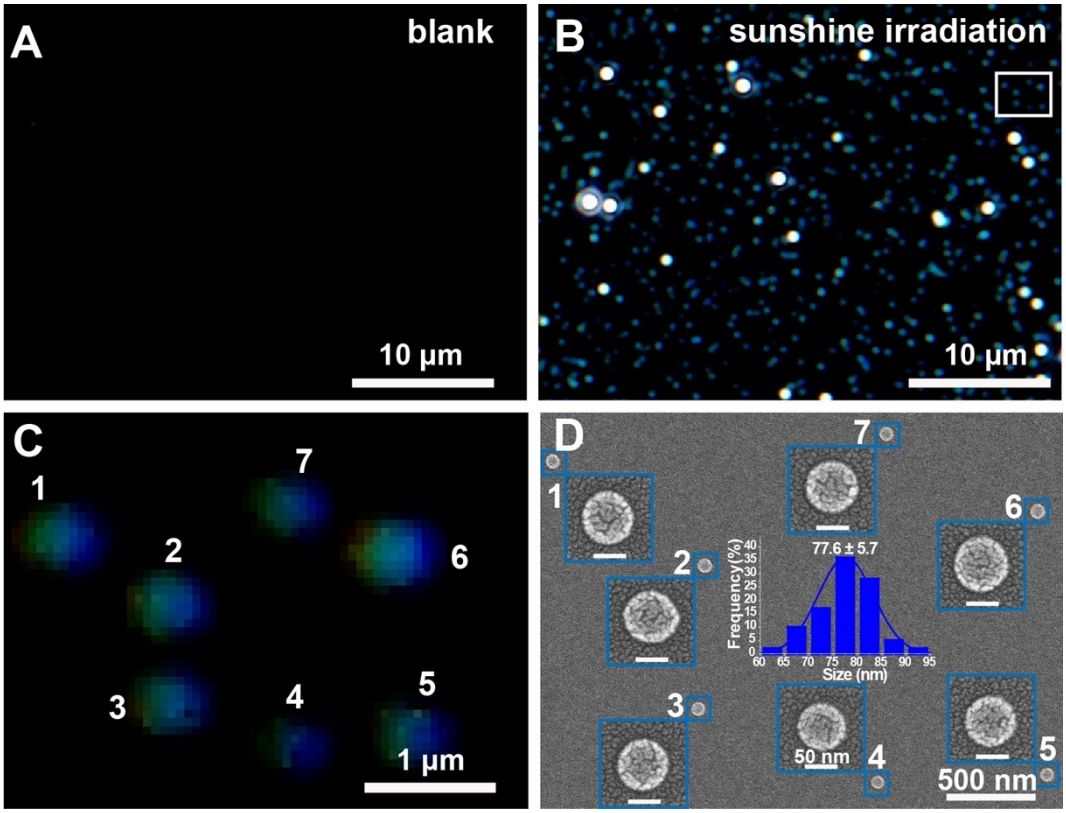

Figure S15 Characterization of organic nanoparticles obtained by photooxidative coupling reaction of *p*-ATP aqueous solution under the irradiation of sunshine. (A) Background DFM image of reaction cell with ultrapure water. (B) DFM images of organic nanoparticles. (C) Magnified DFM image marked with white rectangle in Fig. B. (D) SEM image of the same area in Fig. C, inset is the size distribution of organic nanoparticles (n = 100). $c_{p\text{-ATP}}$, 1×10^{-4} mol·L^{-1}, irradiation time, 60 min, exposure time, 3 s.

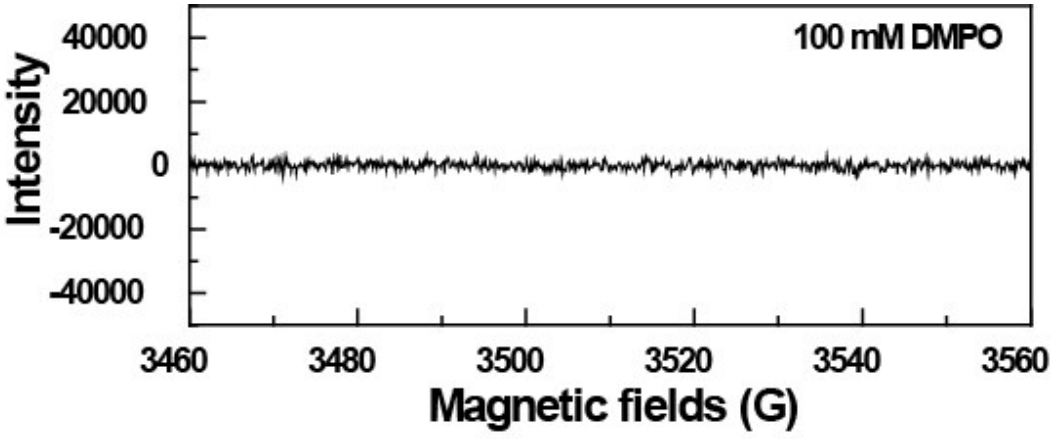

Figure S16 Control EPR spectrum obtained upon incubating 100 mM DMPO in 1:1 water DMF mixture solution without *p*-ATP. spectrometer settings: modulation amplitude, 1.0 G; microwave frequency, 10 GHZ; microwave power, 19 mW; time constant, 10 ms.

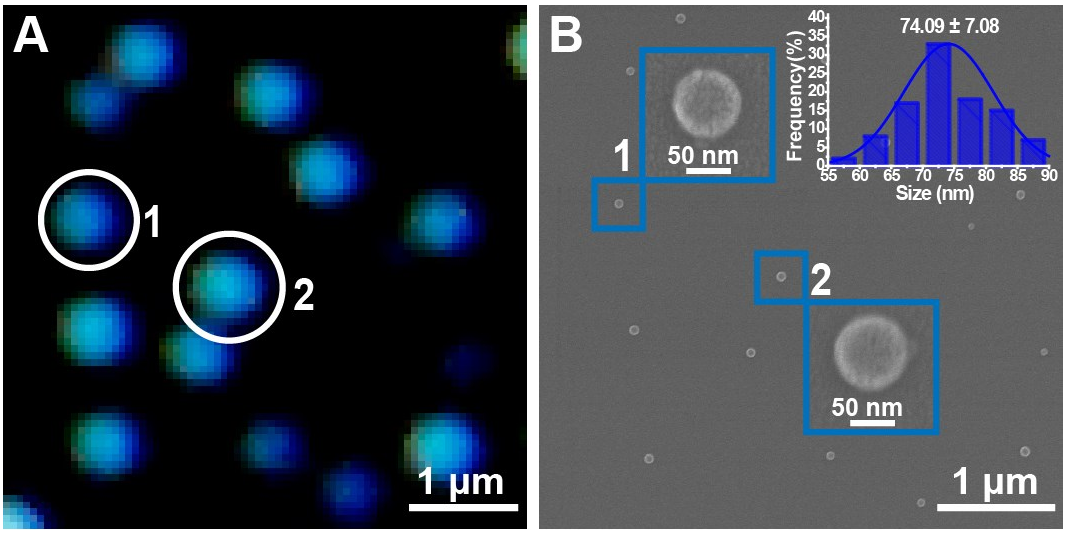

Figure S17 Characterization of photooxidative coupling reaction of *p*-NTP to DPDS. DFM image (A) and SEM image (B) of DPDS organic nanoparticles obtained by irradiation *p*-NTP aqueous solution in dark-field microscope. Inset is the size distribution of organic nanoparticles (n = 100). $c_{p\text{-NTP}}$, 2×10^{-5} mol·L^{-1}, irradiation time, 30 min, exposure time, 3 s.

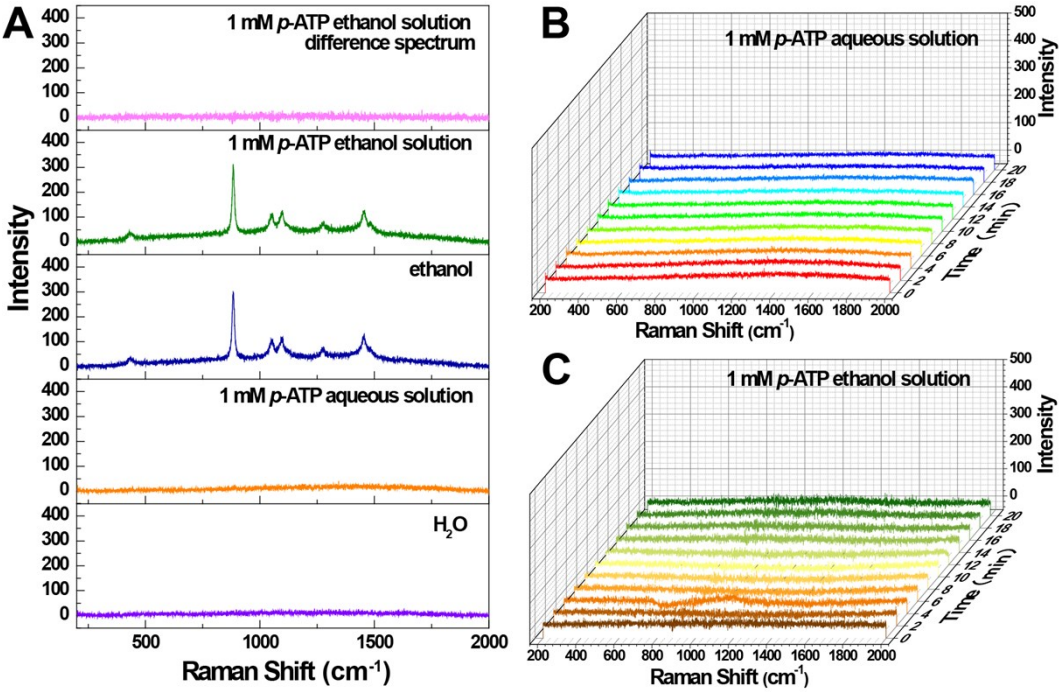

Figure S18 Characterization of photooxidative coupling reaction of *p*-ATP by normal Raman spectroscopy. (A) Normal Raman spectra of the pure solvent (H_2O, ethanol), *p*-ATP solution and difference spectrum of *p*-ATP ethanol solution obtained by subtracting the ethanol spectrum from *p*-ATP ethanol solution spectrum for elimination the interference from ethanol. (B) Evolution of normal Raman spectra of 1 mM *p*-ATP aqueous solution and (C)

Evolution of difference Raman spectra of 1 mM *p*-ATP ethanol solution acquired at different time following 520 nm laser excitation.

References

1 Z. Chi, H. Chen, Q. Zhao and Y. X. Weng, *Nanotechnology*, 2020, **31**, 235712.

2 Y. Liu and C. Z. Huang, *ACS Nano*, 2013, **7**, 11026-11034.

3 Y. F. Huang, M. Zhang, L. B. Zhao, J. M. Feng, D. Y. Wu, B. Ren and Z. Q. Tian, *Angew. Chem. Int. Edit.*, 2014, **53**, 2353-2357.

4 W. Xie and S. Schlücker, *Chem. Commun.*, 2018, **54**, 2326-2336.

5 B. Dong, Y. T. Fang, X. W. Chen, H. X. Xu and M. T. Sun, *Langmuir*, 2011, **27**, 10677-10682.